Two dedicated software, voxel-based, anthropomorphic (torso and head) phantoms.

I. George Zubal, Ph. D., Charles R. Harrell, Eileen O. Smith, B.S., Amy L. Smith

Imaging Science Research Laboratories
Department of Diagnostic Radiology
333 Cedar Street
Yale University School of Medicine, New Haven, CT 06510

ABSTRACT

We have segmented CT torso+head and MRI head slices of two living human males. The manually segmented 129 x-ray CT transverse slices were used to create a computerized 3-dimensional volume array modeling all major internal structures of the body. The original x-ray CT images were reconstructed in a 512x512 matrix with a resolution of 1 millimeter in the x,y plane. The z-axis resolution is 1 centimeter from neck to mid-thigh and 0.5 centimeter from neck to crown of the head. Each voxel of the volume contains an index number designating it as belonging to a given organ or internal structure; 68 such index numbers are assigned. The final torso+head phantom is interpolated to create a 128x128x243 byte volume with isotropic voxel dimensions of 4 mms.

Secondly, a dedicated head phantom was created by similar processing in which 124 transverse MRI were outlined. The transverse T2 slices, recorded in a 256x256 matrix have isotropic voxel dimensions of 1.5mm. This dedicated head phantom contains 62 index numbers designating neurological and taxonomical structures in the brain, as well as anatomical regions. The final volume is contained within a 256x256x128 byte array.

Both of these volume arrays represent high resolution models of the human anatomy and can serve as a voxel-based anthropomorphic phantom suitable for many computer-based modeling and simulation calculations. We have applied them to Monte Carlo simulations from which realistic image projection data has been generated.

INTRODUCTION

Models of the human anatomy serve an important role in several aspects of diagnostic and therapy related image processing. Computerized anthropomorphic phantoms can either be defined by mathematical (analytical) functions, or digital (voxel-based) volume arrays.

One of the earliest computerized anthropomorphic phantoms was developed for estimating doses to various human organs from internal or external sources of radioactivity and served to calculate the S-factors for internal dose calculations in nuclear medicine [1]. This mathematical phantom models internal structures as either ellipsoids, cylinders, or rectangular volumes. For internal dosimetry purposes, such human model approximations serve quite sufficiently and have the advantage of allowing very fast calculation of the intersection of ray lines with the analytical surfaces which delineate the organs. A version of this mathematical phantom has been updated to include female organs [2]. There are additionally versions of the phantom which are used for dedicated cardiac studies where the structures adjacent to the heart and the heart itself have been more realistically modeled [3].

Computer models have also been applied to better understand the image formation process in diagnostic radiology [4-7], particularly for analyzing scatter and attenuation problems in nuclear medicine [8-14]. Since much higher statistics are necessary to model imaging simulations (compared to dosimetry simulations), speed of computing individual gamma ray histories becomes of paramount importance for imaging physics calculations. The software phantoms modeled in these imaging simulations have sometimes been limited to simple point, rod, and slab shapes of sources and attenuating media. Such simple geometries are useful in studying more fundamental issues of scatter and attenuation; but, clinically realistic distributions cannot be adequately evaluated by such simple geometries. The intricate protuberances and convolutions of human internal structures are important in evaluating imaging techniques; and as the resolution of imaging equipment improves, it is essential to enhance our computer models.

In the field of oncology, internal and external radiotherapy sources have become more sophisticated in their design and applications. The calculations involved in clinical therapy planning have become more sophisticated [15-18]. These new therapy techniques can be more effectively investigated with higher resolution, computerized realistic human models.

In order to make 3-dimensional anatomical data suitable for use in any of these radiologic calculations, we must be able to delineate the surfaces and internal volumes which define the various structures of the body. These segmented volumes can then be indexed to activity distributions or other physical characteristics (density or elemental composition). We have constructed an anatomically correct human geometry for use in these types of radiologic calculations where each organ (structure) is segmented and its internal volume is referenced by an index number.

METHODS

Anatomic Data: CT torso+head

Transmission computerized x-ray tomography (CT) supplies us the required high resolution 3-dimensional human anatomy necessary to construct the volume segmented phantom. A considerable number of patients are imaged from head to mid-thigh in our hospital to study diffuse diseases. We selected an adult male whose dimensions were similar the dosimetry standard mathematical phantom [1]. Our selected patient's height was 5 foot 10 inches and weight was 155 pounds. He was scheduled for head, thorax, abdomen, and pelvic scans for diagnosis of diffuse melanoma. The patient had no advanced signs of disease or obvious lesions nor advanced symptoms during the time of the scans. After informing the patient of the potential application of his scans for biomedical research purposes, he agreed to release his scan data for research purposes. The standard clinical imaging protocol was carried out. Using the GE 9800 Quick Scanner, a total of 78 slice images were acquired from neck to mid-thigh with a 1 centimeter slice thickness using a 48 centimeter field of view (pixel size = 1mm). During a second imaging session, 51 slices of the same patient were acquired of the head and neck region with 5 millimeter slice thickness and a field of view of 24 centimeters (pixel size = 0.5mm). The body and head slices were transferred to our image processing lab by reading the reconstructed transverse slices from the CT archive reel to reel magnetic tape, decompressing the images from the manufacturer's lossless storage format, and storing them in expanded matrix format on disk.

Anatomic Data: MRI head

MRI images were acquired on a GE Signa scanner using SPGR mode with FC and 1 nex.

SPGR means spoiled grass (gradient recalled acquisition in the steady state-often called "fast" or "flash"). Volume mode must be used with a grass sequence. Grass acquisitions are generally faster than spin echo sequences and frequently demonstrate better grey/white ratios in the brain. FC stands for flow compensation. It is an option that we put on to elimination any artifact due to moving blood.

The acquisition was stored into a 256x192 matrix size which is interoplated to 256x256 for the Fourier transform.

Organ Delineation

The data access and processing programs were created on a VAX 3500 workstation running VMS version 5.0-2 using the available User Interface Services (UIS routines) for program control of the resident color display screen. The color display monitor is a 1024x1024 pixel raster display equipped with 8 bit planes. One bit plane is used for overlay graphics while the remaining 7 bits are used for mapping 128 color levels to the displayed transverse images. A serial line high resolution Summagraphics bitpad provided high resolution cursor control. An in-house program was developed to read the transverse slices from disk, display them on the color workstation monitor, and permit outlining of organs under bitpad cursor control. The x and y integer positions of all of the organ outlines are stored on disk with a resolution of 512x512 pixels. Members of the medical staff outlined separate internal organs (see Tables 1 and 2) and known structures contained in the transverse slices. A region of interest coloring routine was used to fill the inside of each organ outline with a unique index value. A total of more than three thousand contours were drawn with 1 millimeter resolution to define this fully 3-dimensional voxel phantom of the human and the head. Since the original CT images are still available, the original Hounsfield numbers are also known for each voxel in the defined structures. The scanner used is a clinical instrument; the accuracy of the Hounsfield numbers is assured through the routine maintenance and calibration carried out for quality assurance. Likewise the MRI original slices are also retained so that the original image matrix values can retrieved.

The segmented image information is stored in two independent files. A variable size file is created for each transverse slice and contains the x,y coordinates of each of the contours drawn on that slice. The slice number is retained in the name of the file. These contours serve as the input to the filling routine, which creates a fixed size organ index image. The organ index image is a 512x512 byte matrix filled with integer values which delineate the internal structures (organs) of the body. The organ index image is therefore, in effect, the original CT transverse slice in which the Hounsfield numbers or the original MRI T2 values are replaced by integers corresponding to the organ index value. The assignment of integers to the organs are shown in Table 1 and 2.

Data Archive

The total storage capacity of the files are: original CT images = 29 Megabyte, x,y contours = 1 Megabyte, organ index matrices 20 Megabytes; original MRI images = 36 Megabytes. x. y contours = 3 Megabytes, organ index matrices = 28 Megabytes and are available for public access through our Imaging Processing and Analysis Laboratory. To gain access to the data, send a request to Dr. George Zubal e-mail: Zubal@BioMed.Med.Yale.Edu.

RESULTS

In order to appreciate some of the internal detail of the voxel based phantoms, we present two figures in which slices out of the torso+head and head phantom are shown. Figure 1 shows a transverse, coronal, and sagittal slice through the complete torso+head phantom. Figure 2 shows an original MRI slice from the head phantom with orange overlay contours showing the manual segmentation of this selected slice; to the right we see this same slice filled with various colors delineating various internal structures. The small boxes seen in this figure can be best understood as "handles" by which an individual contour can be individually selected by the computer cursor.

CT Torso+Head Phantom

The files that are contained under this area are of 3 types.

1. Raw CT data files these files are copy of a GE 9 track tape. These files are compressed. But can be uncompressed into a 512x512 two-byte signed integer array. Depending upon hardware, these two-byte words may need to be swapped before displaying.
2. Color data slices, these files are compressedand can be expanded to a 512x512 one-byte array. The head and torso of the torso+head phantom are stored separately. Each byte represents a pixel with a corresponding value. For the head, slice #1 starts at the neck and slice #56 ends at the top of the head. For the body, slice #1 starts at the neck and slice #78 ends at the mid-thigh.
3. Uncompressed colored data files are not compressed. Access as a 128x128x243 one-byte array. There are a total of 243 slices in this volume with each slice having a dimension of 128x128 bytes. The complete torso+head phantom is combined.

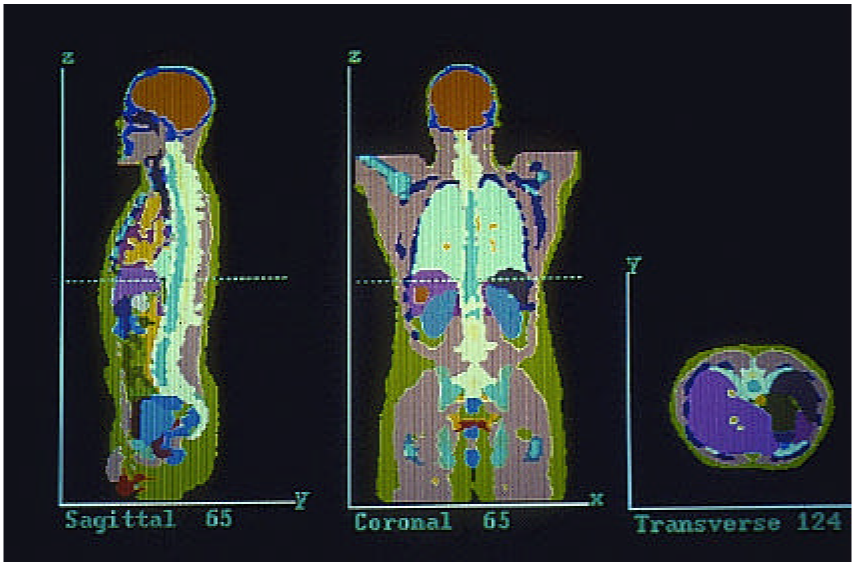

Figure 1: Saggital, coronal, and transverse slice through the voxel-based phantom.

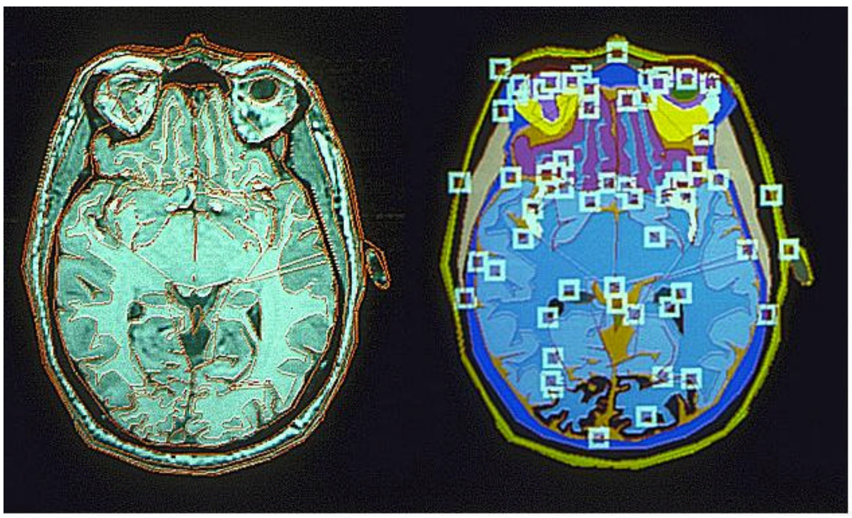

Figure 2: An selected original MRI T2 image with overlay of contours drawn for segmenting internal structures (left). Arbitrary color designation of internal brain structures (right); small squares are used for contour selection via screen cursor.

The raw CT imaging was done in two parts. The head was acquired at 5 mm per slice, and approximately 0.5mm resolution in x y plane. The body was done 10 mm / slice, and 1 mm resolution in the x y plane. The composite data set was created by attaching the colored head slices onto the body. We first extratced the center 256x256 pixels from the head slices, and then expaded to 512x512 to yield the proper 1 mm x y plane resolution. The next step was to find the slices that most closely matched between the head and the body, and align them. The first body slice was matched to slice 11 of the head, so we used slices 56 thru

11 of the head data set. The offset measured between the two data sets was 10 pixels in the x dimension, and 20 pixels in the y dimension.

After the data sets had been aligned, we compressed the x,y dimensions, and duplicated slices to get symmetric voxels of 2.5 mm, using a median compression scheme. The head was then placed on the body a 3 dimensional median filter was run over the data set to remove "boxiness" caused by duplicating slices. The filter was 3x3x3.

In the original color slices the organ numbers are offset from 0 by 63 so the values for skin etc start at 64 thru 126. The 0 for outside of phantom remains fixed. The organ numbers have all been shifted down for the composite phantom, and expanded to the list actually shown below.

MRI-based Brain Phantom

The segmented brain phantom is made from 124 MRI slices of a brain. The original MRI's are 256x256 two-byte words, but the "colored" slices are 256x256 one-byte array. The slice spacing is 1.4 mm the pixel size in the x y plane is 1.09 mm. Three data sets have been stored.

1. Raw MRI data files are compressedand expand into a 256x256 two-byte signed integer array. Depending upon hardware, these two-byte words may need to be swapped before displaying these MRI slices.

2. Color data slices these files are compressed and expendable to a 256x256 one-byte array. Each byte represents a pixel with a corresponding value. For the head, slice #1 starts at the roof of mouth and slice #120 ends at the top of the head.

3. Uncompressed colored data file is not compressedand is stored as a 256x256x128 one-byte array. There are a total of 128 slices in this volume, the first and last 4 slices are blanks.

Colored slices are organs maps where each organ has been assigned a specific value. For example the tongue would have a value of 77 assigned to it. This means that where ever tongue appears in the raw MRIs, a number 77 has been placed in the colored slices.

Table 1 CT based torso-head phantom

organ id *c.dat	organ id *.dat	organ
0	0	outside phantom
64	1	skin
65	2	brain
66	3	spinal cord
67	4	skull
68	5	spine
69	6	rib cage & sternum
70	7	pelvis
71	8	long bones
72	9	skeletal muscle
73	10	lungs
74	11	heart
75	12	liver
76	13	gall bladder
77	14	kidney
80	17	stomach
81	18	small bowel
82	19	colon
83	20	pancreas
84	21	adrenals
87	24	gas (bowel)
88	25	fluid (bowel)
90	27	lymph nodes
91	28	thyroid
94	31	spleen
95	32	urine
96	33	feces
97	34	testes
98	35	prostate
100	37	rectum
102	39	diaphragm
103	40	bladder
126	63	lesion
69	70	dens of axis
70	71	jaw bone
73	74	lacrimal glands
74	75	spinal canal
75	76	hard palate
76	77	cerebellum
77	78	tongue
78	15	pharynx
79	16	esophagus
84	85	medulla oblongota
85	22	fat
86	23	blood pool
89	26	bone marrow
90	91	pons
92	29	trachea
93	30	cartilage
98	99	uncus(ear bones)
103	104	sinuses / mouth cavity
105	106	optic nerve
112	113	cerebral falx
118	119	eye
120	121	lens
121	122	cerebral aquaduct
124	125	teeth

Table 2 MRI head phantom

organ id *.c files	organ id MRI_brain	organ
0	0	outside phantom
64	1	skin
65	2	brain
66	3	spinal cord
67	4	skull
68	5	spine
69	70	dens of axis
70	71	jaw bone
71	72	parotid gland
72	9	skeletal muscle
73	74	lacrimal glands
74	75	spinal canal
75	76	hard palate
76	77	cerebellum
77	78	tongue
78	15	pharynx
79	16	esophagus
80	81	horn of mandible
81	82	nasal septum
82	83	white matter
83	84	superior sagital sinus
84	85	medulla oblongota
85	22	fat
86	23	blood pool
87	88	artificial lesion
88	89	frontal lobes
89	26	bone marrow
90	91	pons
91	92	third ventricle
92	29	trachea
93	30	cartilage
94	95	occipital lobes
95	96	hippocampus
96	97	pituitary gland
97	98	cerebral fluid
98	99	uncus(ear bones)
99	100	turbinates
100	101	caudate nucleus
101	102	zygoma
102	103	insula cortex
103	104	sinuses / mouth cavity
104	105	putamen
105	106	optic nerve
106	107	internal capsul
107	108	septum pellucidium
108	109	thalamus
109	110	eyeball
110	111	corpus collosum
111	112	special region frontal lobes
112	113	cerebral falx
113	114	temporal lobes
114	115	fourth ventricle
115	116	frontal portion eyes
116	117	parietal lobes
117	118	amygdala
118	119	eye
119	120	globus pallidus
120	121	lens
121	122	cerebral aquaduct
122	123	lateral ventricles
123	124	prefrontal lobes
124	125	teeth
126	63	lesion

DISCUSSION

We have created a digital voxel-based phantom which closely resembles a typical male anatomy. Organ outlines were manually drawn with millimeter resolution in each of 129 transverse slice images of the human torso. Such an anthropomorphic 3-dimensional phantom has several interesting applications in the radiological sciences. We have routinely used the voxel based phantom in Monte Carlo simulations to yield diagnostically realistic images of internal distributions of radiopharmaceuticals [19,20]. Since we are able to model a known source distribution and known attenuator distribution, the Monte Carlo simulations give us projection data which not only closely resemble clinical data, but include additional information not determinable in patient studies. Such data sets can help to better understand the image formation process for clinically realistic models, and can prove especially interesting in testing and improving tomographic reconstruction algorithms [21].

New imaging devices can be investigated using "in vivo" simulations. The tumor detection capabilities of a novel coincidence counting probe system has been investigating using the anthropomorphic phantom described here [22]. Early design changes can be realized before studies are conducted in living models. One of the advantages of developing this very realistic human model is that such simulations can decrease the necessity of conducting experimental studies using animal models - particularly primates.

Dose calculations for internal and external radiation sources using this phantom can give new insights in the field of health physics and therapy. We hope to extend the application of this phantom to therapy related simulations.

ACKNOWLEDGEMENTS

Work performed under Contract No. DE FG02-88ER60724 with the U.S. Department of Energy. We are thankful to Mindy Lee, whose computer programming skills were essential for outlining and storing the segmented data. We are indebted to Cornelius N. de Graaf Utrecht, The Netherlands, for his implementation of the volumetric smoothing.

REFERENCES

[l] W Snyder, MR Ford, G Warner: *Estimates of Specific Absorbed Fractions for Photon Sources Uniformly Distributed in Various Organs of a Heterogeneous phantom.* NM/MIRD Pamphlet No. 5., (Society of Nuclear Medicine Publication., New York, 1978).

[2] G Williams, M Zankl, W Abmayr, R Veit, G Drexler: "The Calculation of Dose from External Photon Exposures using Reference and Realistic Human Phantoms and Monte Carlo Methods", Phys. Med. Bio.,**31**, 449-452, (1986).

[3] H. Wang, RJ Jaszczak, RE Coleman: "Solid Geometry-Based Object Model for Monte Carlo Simulated Emission and Transmission Tomographic Imaging Systems." IEEE Transactions on Medical Imaging,**11**, 361-372, (1992).

[4] G Barnea, CE Dick: "Monte Carlo studies of x-ray scatterings in transmission diagnostic radiology." Med. Phys.,**16**,: 490-5, (1986).

[5] HP Chan, K Doi: "Physical characteristics of scattered radiation in diagnostic radiology: Monte Carlo simulation studies." Med. Phys.,**12,** 152-65, (1985).

[6] H Kanamori, N Nakamori, K Inone: "Effects of Scattered x-rays on CT images." Phys. Med. Bio.,**30,** 239-49, (1985).

[7] DR Dance, GJ Day: "The computation of scatter in mammography by Monte Carlo methods." Phys. Med. Bio.,**29**, 237-47, (1984).

[8J J Logan, HJ Bernstein: "A Monte Carlo simulation of Compton scattering in positron emission tomography." J. Comput. Assist. Tomogr.,**7**, 316-20, (1983).

[9] CE Floyd, RS Jaszczak, CC Harris, RE Coleman: "Energy and spatial distribution of multiple order Compton scatter in SPECT. A Monte Carlo investigation." Phys. Med. Bio.,**29,** 1217-30, (1984).

[10] CE Floyd, RJ Jaszczak, KL Greer, RE Coleman: "Deconvolution of Compton scatter in SPECT." J. Nucl. Med.,**26,** 403-8, (1985).

[11] CE Floyd, RJ Jaszczak, KL Greer, RE Coleman: "Inverse Monte Carlo as a Unified Reconstruction Algorithm for ECT." J. Nucl. Med.,**27,** 1577-85, (1986).

[12] CE Floyd, RJ Jaszczak, KL Greer, RE Coleman: "Brain Phantom: high resolution imaging with SPECT and I-123." Radiology,**164**, 279-81, (1987).

[13] JW Beck, RJ Jaszczak, RE Coleman, CF Starmer, LW Nolte. "Analysis of SPECT Including Scatter and Attenuation Using Sophisticated Monte Carlo Modeling Methods." IEEE Transactions on Nuclear Science,**29**, 506-511, (1982).

[14] D Acchiappati, N Cerullo, R Guzzardi: "Assessment of the Scatter Fraction Evaluation Methodology using Monte-Carlo Simulation Techniques." European Journal of Nuclear Medicine,**15**, 683-686,(1989).

[15] M Saxner, A Trepp, A Ahnesjo: "A pencil beam model for photon dose calculation." Med. Phys.,**19**, p 263-273, (1992).

[16] AS Meigooni, R Nath: "Tissue inhomogeneity correction for brachytherapy sources in a heterogeneous phantom with cylindrical symmetry." Med. Phys.,**19,** 401-407, (1992).

[17] R Mohan, G Mageras, B Baldwin, L Brewster, G Kutcher, S Leibel, C Burman, C. Long, Z Fuks: "Clinically relevant optimization of 3-D conformal treatments." Med. Phys.,**19**, 933-944, (1992).

[18] D Nigg, P Randolph, F Wheeler: "Demonstration of three-dimensional deterministic radiation transport theory dose distribution analysis for boron neutron capture therapy." Med. Phys.,**18,** 43-53, (1991).

[19] IG Zubal, CH Harell. "Voxel based Monte Carlo Calculations of Nuclear Medicine Images and Applied Variance Reduction Techniques." Image and Vision Computing,**10,** 342-348, (1992).

[20] IG Zubal, CR Harrell, PD Esser. "Monte Carlo determination of emerging energy spectra for diagnostically realistic radiopharmaceutical distributions." Nuclear Instruments and Methods in Physics Research, **A299,** 544-547,(1990).

[21] GS Hademenos, MA King, M Ljungberg, IG Zubal, CR Harrell. "A Scatter Correction Method for T1201 Images: A Monte Carlo Investigation." *1992 IEEE Nuclear & Science Symposium and Medical Imaging Conference* Oct. 25-31, 1992, Orlando FL, Volume 2, pp. 1213-1216.

[22] JR Saffer, HH Barrett, HB Barber , JM Woolfenden. "Surgical Probe Design for a coincidence Imaging System Without a Collimator" *Proceeding of the 12th International Conference on Information Processing in Medical Imaging*,, Springer-Verlag, Ed Colchester and Hawkes, 8-22, (1991).